Available online at www.sciencedirect.com
ScienceDirect
Physica B 403 (2008) 2431–2437
PHYSICA B
www.elsevier.com/locate/physb

The effect of the post-annealing temperature on the nano-structure and energy band gap of SnO_2 semiconducting oxide nano-particles synthesized by polymerizing–complexing sol–gel method

M.-M. Bagheri-Mohagheghi[a,b,*], N. Shahtahmasebi[a], M.R. Alinejad[a], A. Youssefi[c], M. Shokooh-Saremi[d]

[a]*Department of Physics, School of Basic Sciences, Ferdowsi University of Mashhad, Mashhad, Iran*
[b]*Department of Physics, Damghan University of Basic Sciences, Damghan, Iran*
[c]*Par-e-Tavoos Research Institute, Nanotechnology Laboratory, Mashhad, Iran*
[d]*Department of Electrical and Computer Engineering, University of Connecticut, Storrs, CT 06269-2157, USA*

Received 18 December 2007; received in revised form 1 January 2008; accepted 3 January 2008

Abstract

Nano-crystalline SnO_2 particles have been synthesized by sol–gel process using a simple starting hydro-alcoholic solution consisting of $SnCl_4$, $5H_2O$ and citric acid as complexing and ethylene glycol as polymerization agents. The structural properties of the prepared tin oxide nano-powders annealed at different temperatures (300–700 °C) have been characterized by X-ray diffraction (XRD) and transmission electron microscopy (TEM) analyses. The XRD patterns show SnO_2-cassiterite phase in the nano-powders, and size of crystals increases by increasing the annealing temperatures. The TEM images show nano-particles as clusters with size in the range of 5–25 nm. Electron diffraction pattern of nano-powders annealed at different temperatures shows a homogeneous distribution of spherical particles due to the effect of ethylene glycol as polymerizing agent in sol–gel process. The optical direct band gap values of SnO_2 nano-particles were calculated to be about 4.05–4.11 eV in the temperature range 300–700 °C by optical absorption measurements. These values exibit nearly a 0.5 eV blue shift from that of bulk SnO_2 (3.6 eV), which is related to size decrease of the particles and reaching to the quantum confinement limit of nano-particles.

PACS: 78.67.Bf; 61.46.Df; 61.05.Cp

Keywords: Tin oxide; Nano-particle; Sol–gel method; Annealing temperature

1. Introduction

Tin oxide (SnO_2), with cassiterite structure, as bulk or thin films is a wide band gap n-type semiconductor ($E_g = 3.6$–3.8 eV), known as one of the most widely used semiconducting oxides due to its chemical and mechanical stabilities. It has been widely studied over decades because of its most applications in various solid state and ceramic devices, sensors, optoelectronics and catalysis [1–6]. Among the technical applications, the most important uses of SnO_2 are as gas sensors, bulk ceramics, glaze and pigments. On the other hand, the majority of chemical and physical properties of SnO_2 material depend on the number of structural parameters. For example, the sensing properties of SnO_2 sensors (sensitivity, selectivity and reproductively) critically depend on some features, mainly particle size and specific surface area. Therefore, preparation of primary powders as nono-particles increases specific surface area of the particles and hence improves the efficiency function of the sensor [1,5–7]. Due to these modifications,

*Corresponding author at: Department of Physics, School of Basic Sciences, Ferdowsi University of Mashhad, P.O. Box: 91375-4889, Mashhad, Iran. Tel.: +98 511 8545151; fax: +98 511 8546571.
E-mail addresses: bmohagheghi@dubs.ac.ir, m_mohagheghee@yahoo.co.uk (M.-M. Bagheri-Mohagheghi), saremi@engr.uconn.edu (M. Shokooh-Saremi).

0921-4526/$ - see front matter © 2008 Elsevier B.V. All rights reserved.
doi:10.1016/j.physb.2008.01.004

application of nano-structured SnO_2 as an active material in gas sensor is well known.

Along with the different wet chemical methods of preparing nano-particle SnO_2, sol–gel [4,6,8], precipitation [9,10], hydrothermal route [10,11] and spray pyrolysis [12,13] are well recognized. Recently, polymerizing–complexing (PC) combustion method, which is a modified Pechini process [14,15], without any precipitation, has been used for preparation of semiconducting nano-particles, like SnO_2. This method consists of a variety of organic fuels such as citric acid, urea, hydrazine, EDTA and polyethylene glycol as complexing or polymerization agent [7,16]. Indeed, PC method provides more homogeneous fine powder than any other techniques with immobilization of metal–chelate complexes and forming stable metal complexes via increasing the polymerization.

However, preparation of nano-particles of metal oxides at low cost in industrial scale is a challenge in material production. So, using the cheap materials, simple fabrication processes and suitable conditions of synthesis are the main requirement for this process. Therefore, the study of influence of various parameters such as initial solution combination, time and temperature of heat treatments, and type of complexing and polymerizing agents is very important for nano-powders production.

The main purpose of the present research is to study the post-annealing temperature effect on nano-particle size, nano-structure and energy band gap of SnO_2 powders synthesized by the PC sol–gel method.

2. Experimental procedure

2.1. Synthesis of SnO_2 nano-powders

SnO_2 nano-powder synthesization by the PC method is summarized in a flow chart shown in Fig. 1. First, the initial sol consisting of $SnCl_4$ and $5H_2O$, H_2O and ethanol with equal weight percentage is prepared. Then, citrate acid and ethylene glycol subsequently added to this solution, and the resulting mixture was stirred and dissolved at 40 °C for 20 min until a completely clear solution was obtained. The obtained solution was refluxed at $T = 120$ °C for 3 h. During refluxing the solution turned into a metal–citrate homogeneous complex with a little color change from clear to light yellow. After cooling down, in order to bring about the required chemical reactions for the development of polymerization and evaporation of the solvent, the sol was further slowly heated at $T = 80 \pm 5$ °C for 20 h in an open bath until a brown-yellow wet gel was obtained. During continuous heating at this temperature, the polymerization between citrate acid, ethylene glycol and complexes is developed, and finally sol became more viscous as a wet gel. In the final step of sol–gel process, the wet gel was fully dried by direct heating on the hot plate at $T = 150$ °C for 4 h. The resultant production was a black-brown porous gel as airogel.

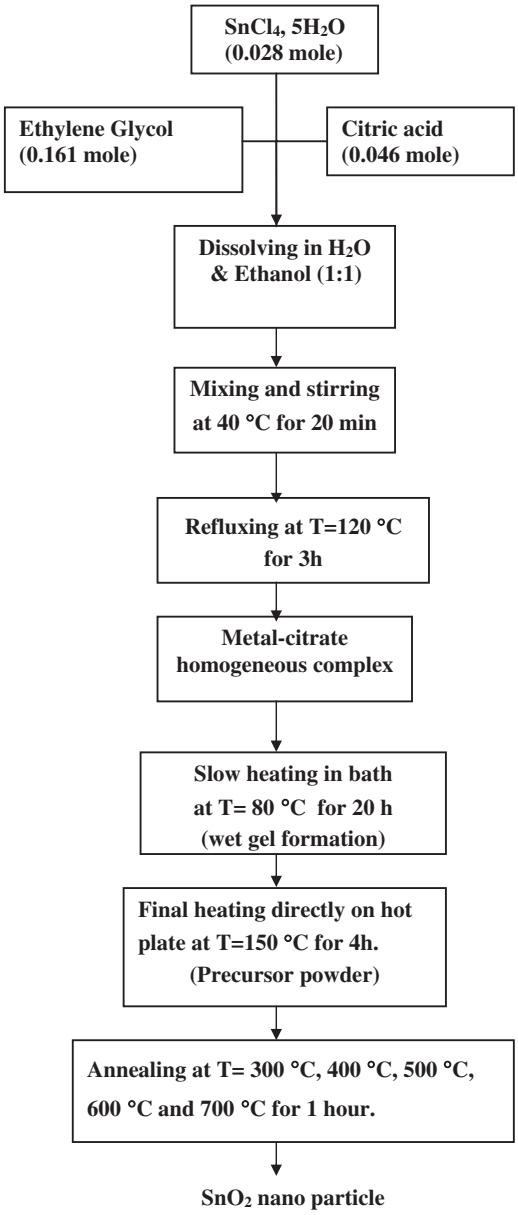

Fig. 1. The flow chart of preparation of SnO_2 nano-particles by sol–gel process.

2.2. Post-annealing of SnO_2 nano-powders at different temperatures

The precursor powder (xerogel), which has been prepared by grinding airogel, was annealed at 300–700 °C for 1 h (in air) in glassy boat in an electric box furnace and then cooled down to room temperature. The weight reduction results of annealed powders were given in Table 1.

2.3. Characterization of powders

The X-ray diffraction (XRD) patterns of SnO_2 nano-crystals prepared at various annealing temperatures were recorded by the D8 Advance Bruker system using CuKα

($\lambda = 0.154056$ nm) radiation with 2θ in the range 20–70°. Transmission electron microscopy (TEM) micrographs and electron diffraction patterns of the prepared SnO_2 nano-powders were recorded by the LEO system (model 912 AB) operating at 120 kV. The required samples for TEM analysis was prepared by dispersing the SnO_2 nano-powders in acetone using an ultrasound bath. A drop of this dispersed suspension was put onto 200-mesh carbon-coated Cu grid and then dried in vacuum. Also, the optical absorption measurements of nano-powders in range of 190–450 nm were recorded using a UV–VIS single beam spectrophotometer (Agilent 8453) for calculating optical band gap values.

3. Results and discussion

Table 1 shows the results of post-annealing of powders at different temperatures. As observed, by increasing the annealing temperature from 300 to 500 °C, a rapid mass loss of powders occurs due to evaporation and removing organic additives such as citrate acids and ethylene glycol. The most mass reduction occurs in $T = 500$ °C and higher

Table 1
The weight results of annealed of SnO_2 powders at different temperatures

Sample	Annealing temperature, T_a, for 1 h (°C)	Weight (g) (before heating)	Weight (g) (after heating)	Weight reduction (Δw) (%)	Size range of particles (by TEM) (nm)
1	300	1.7	1.17	31.17	4–14
2	400	1.7	0.79	53.52	–
3	500	1.7	0.397	76.6	5–20
4	600	1.7	0.397	76.6	–
5	700	1.7	0.397	76.6	15–25

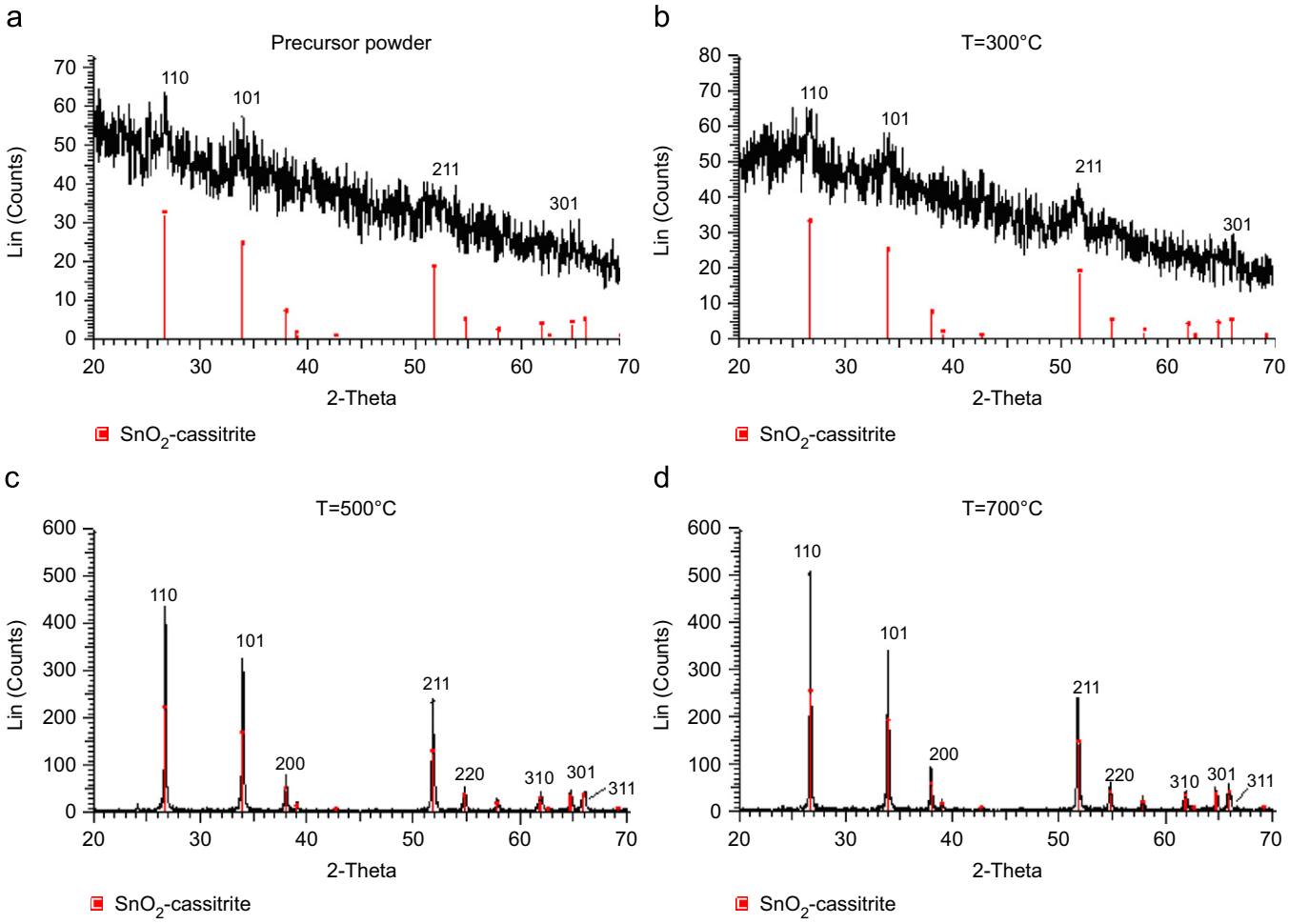

Fig. 2. The XRD patterns of the SnO_2 nano-particles annealed at different temperatures, (a) dry gel-powder, (b) 300 °C, (c) 500 °C and (d) 700 °C.

Table 2
The XRD parameters and mean size of particles in different crystallography orientations at different annealing temperatures

hkl	2θ (deg)	*D* (Å)	Intensity Lin (Cps)	FWHM 2θ (deg)	Particle mean size, D (nm)	Identification with (*h k l*) value
T = dry gel (T = 150 °C)						
110	26.705	3.33	64.1	0.252	6.28	Tetragonal SnO_2
101	33.948	2.63	58.1	0.283	5.69	Tetragonal SnO_2
211	51.89	1.76	42.6	0.342	5.01	Tetragonal SnO_2
T = 300 °C						
110	26.702	3.33	66.2	0.191	8.29	Tetragonal SnO_2
101	33.943	2.63	59.2	0.223	7.22	Tetragonal SnO_2
211	51.86	1.76	44.1	0.272	6.37	Tetragonal SnO_2
T = 500 °C						
110	26.652	3.34	353	0.113	14.01	Tetragonal SnO_2
101	33.939	2.63	269	0.136	11.83	Tetragonal SnO_2
200	37.99	2.36	65.6	0.091	17.91	Tetragonal SnO_2
211	51.81	1.76	192	0.147	11.78	Tetragonal SnO_2
220	54.847	1.67	41.2	0.199	8.72	Tetragonal SnO_2
T = 700 °C						
110	26.584	3.35	405	0.106	14.93	Tetragonal SnO_2
101	33.868	2.64	291	0.106	15.18	Tetragonal SnO_2
200	37.94	2.36	79.2	0.119	13.69	Tetragonal SnO_2
211	51.757	1.76	212	0.133	13.02	Tetragonal SnO_2
220	54.766	1.67	51.3	0.12	14.47	Tetragonal SnO_2

temperatures ($\Delta w = 76.6\%$). This indicates that all the organic additives are removed from powders by annealing at $T = 500\,^{\circ}C$.

The XRD patterns of prepared SnO_2 nano-powders at different annealing temperatures are shown in Fig. 2(a)–(d). It is clear that the powders which are not annealed (Fig. 2(a)) and these annealed at $T = 300\,^{\circ}C$ (Fig. 2(b)) are slightly crystalline with a great amorphous background. Those annealed at $T = 500$ and $700\,^{\circ}C$ are completely crystallized (Fig. 2(c) and (d)). Certainly, crystallization starts at $T = 300\,^{\circ}C$ and amorphous background falls down. Also, the Bragg's peaks of the crystallized powders correspond to each sample agree well with the reflections of pure tetragonal SnO_2 single phase (cassiterite) with $a = 4.74\,Å$ and $c = 3.19\,Å$. The XRD patterns at all annealing temperatures show that the intensities of three basic peaks of the (1 1 0), (1 0 1) and (2 1 1) planes are more than of other peaks.

Table 2 shows the XRD parameters and mean size of the SnO_2 nano-particles in various crystalline orientations at different annealing temperatures. As seen in Table 2, the width of the peaks decreases with increasing annealing temperature, $T \geqslant 300\,^{\circ}C$, which refers to the growth of crystals size and construction of larger clusters. The mean size of nano-particles was also calculated using the Scherrer formula based on the XRD patterns [1]

$$D = K\lambda/\delta w \cos\theta, \quad (1)$$

where D is the mean size of particle, K is a constant (~ 1), λ is the X-ray wavelength ($K\alpha(Cu) = 0.154056\,nm$), δw is the full-width at half-maximum (FWHM) of XRD peaks and θ is the Bragg's angle.

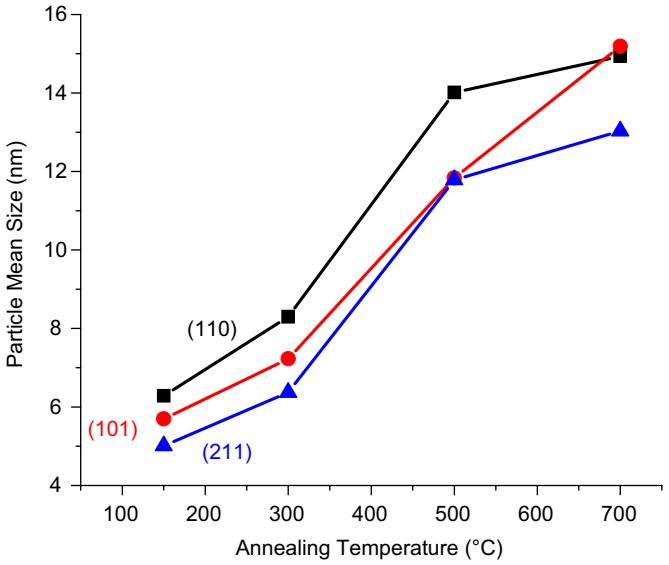

Fig. 3. The dependence of particles size at annealing temperature in crystalline orientations of (1 1 0), (1 0 1) and (2 1 1).

The temperature dependence of particles size in crystalline orientations of (1 1 0), (1 0 1) and (2 1 1), based on Table 2, is shown in Fig. 3, which indicates that the mean size of nano-particles has increased in the range of 5–16 nm with increase in annealing temperature, especially in (1 1 0) orientation.

The TEM micrographs of the SnO_2 nano-powders annealed at different temperatures are shown in Fig. 4. The TEM images confirm the nanometric size of the particles in the range of 5–25 nm depending on the annealing temperature. Fig. 4(a) exhibits nano-sized SnO_2

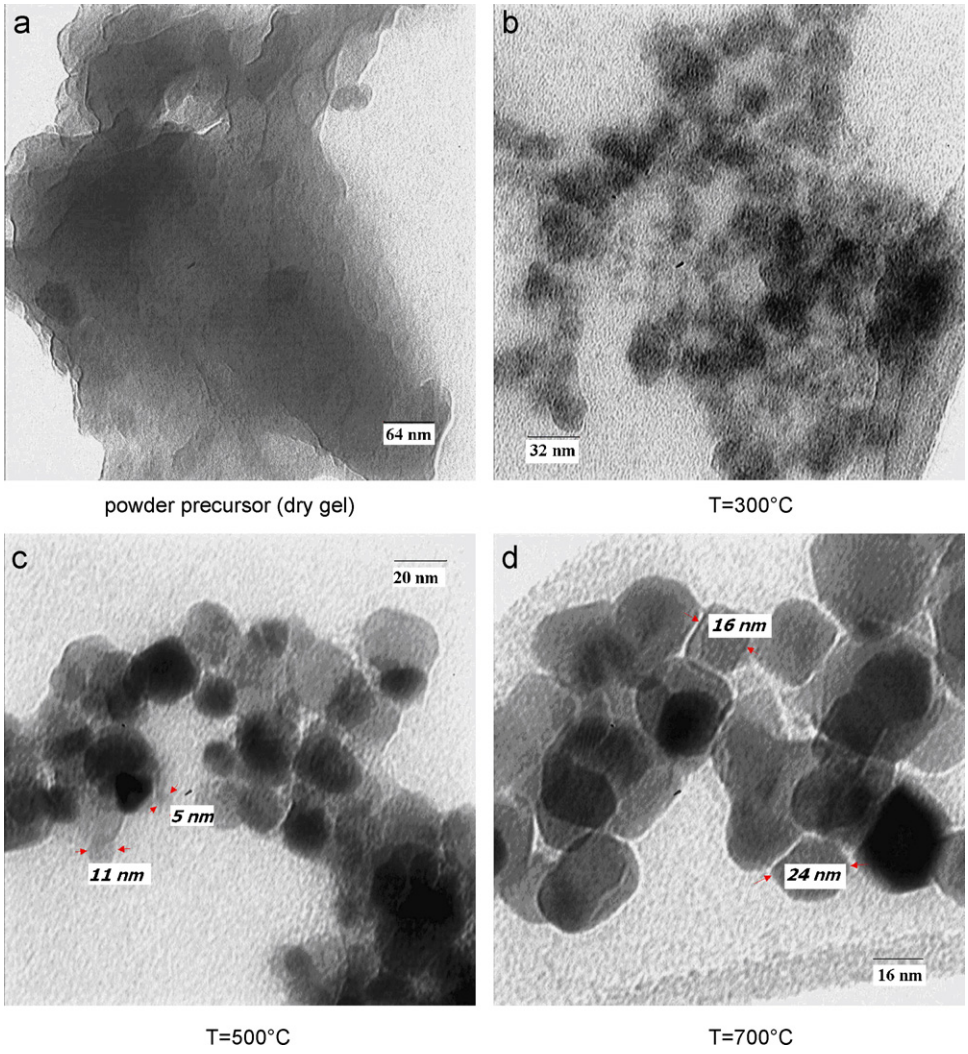

Fig. 4. The TEM images of SnO_2 nano-particles annealed at different temperatures, (a) dry gel-powder, (b) $T = 300\,^{\circ}C$, (c) $T = 500\,^{\circ}C$ and (d) $T = 700\,^{\circ}C$.

particles inside a dark background due to the organic additives maintenance, i.e. citrate acid and ethylene glycol, in the powder. By increasing the calcination temperatures above 500 °C, the dark background is completely removed, and nano-crystals are observed completely, as shown in Fig. 4(b)–(d).

In addition, the morphology of SnO_2 nano-crystals strongly depends on the annealing temperatures, so that in higher temperatures, especially in $T \geqslant 500\,^{\circ}C$, the size of nano-crystals with tetragonal structure is increased, as shown in Fig. 4(c) and (d). The TEM micrograph of powders also shows a homogeneous distribution of nano-particles in powders, basically, due to the addition of ethylene glycol as polymerization agent to precursor solution and its effect on homogeneous distribution of nano-particles.

These results indicate that citrate acid and ethylene glycol are more effective for homogeneous atomization of Sn cations in xerogel or prevent from the agglomeration and grain growth of SnO_2 particles. Indeed, in the PC based sol–gel method, the complexing ligands can cover particles and prevent from their agglomeration [1,4,16].

The selected area electron diffraction (SAED) patterns of nano-particles in different calcinations temperatures are shown in Fig. 5(a)–(d). The electron diffraction patterns of nano-particles represent a collection of halo-rings and discrete spots, and confirm poly-crystalline structure of the prepared nano-particles. By increasing annealing temperature and particle size, at $T \geqslant 300\,^{\circ}C$, electron diffraction patterns become more sharpened. On the other hand, the structure of particles tends from disorderly separate fine particles to crystalline structure with well-orientated crystals, as shown in Fig. 5(c) and (d). The (SAED) patterns also show a homogeneous distribution of particles that can be attributed to the use of ethylene glycol as polymerizing agent in sol–gel synthesis [4,17].

The direct band gap values of the SnO_2 nano-particles prepared by sol–gel method are presented in Fig. 6(a)–(d). The data for Fig. 6 are obtained by optical absorption measurements and plotting $(\alpha h\nu)^2$ versus photon energy

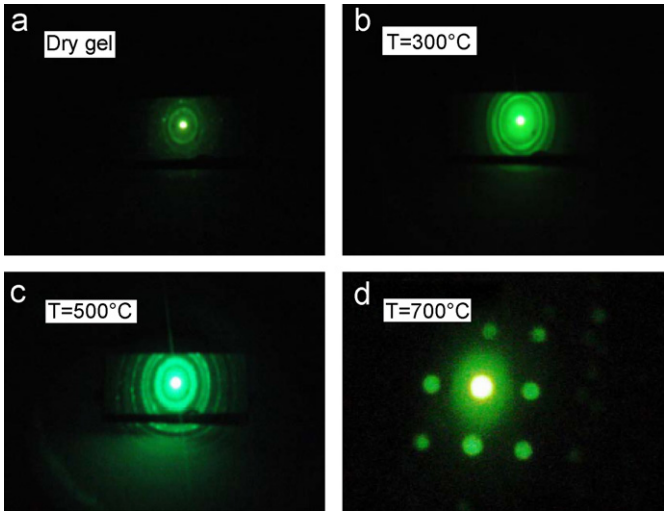

Fig. 5. The electron diffraction patterns of SnO_2 nano-particles annealed at different temperatures, (a) dry gel-powder, (b) $T = 300\,^{\circ}C$, (c) $T = 500\,^{\circ}C$ and (d) $T = 700\,^{\circ}C$.

($h\nu$) using the following relation for direct energy gap [18]:

$$(\alpha h\nu)^2 = A(h\nu - E_g), \tag{2}$$

where α is the absorption coefficient, A and E_g are constant and band gap of the material, respectively.

As illustrated in Fig. 6(a)–(d), in region $T \geqslant 300\,^{\circ}C$, the optical direct band gap values of nano-particles have changed from 4.05 to 4.11 eV by increasing the annealing temperature. These values exhibit an almost 0.5 eV blue shift from that of bulk SnO_2 (3.6 eV), which is related to the size decrease of particles and we attribute it to the quantum confinement limit reaching of nano-particles. The quantum confinement effect is expected for semiconducting nano-particles, and the absorption edge will be shifted to a higher energy when the particle size decreases [18]. In addition, the value of band gap for dry gel is 3.32 eV, which is related to the organic additive remains in the powder.

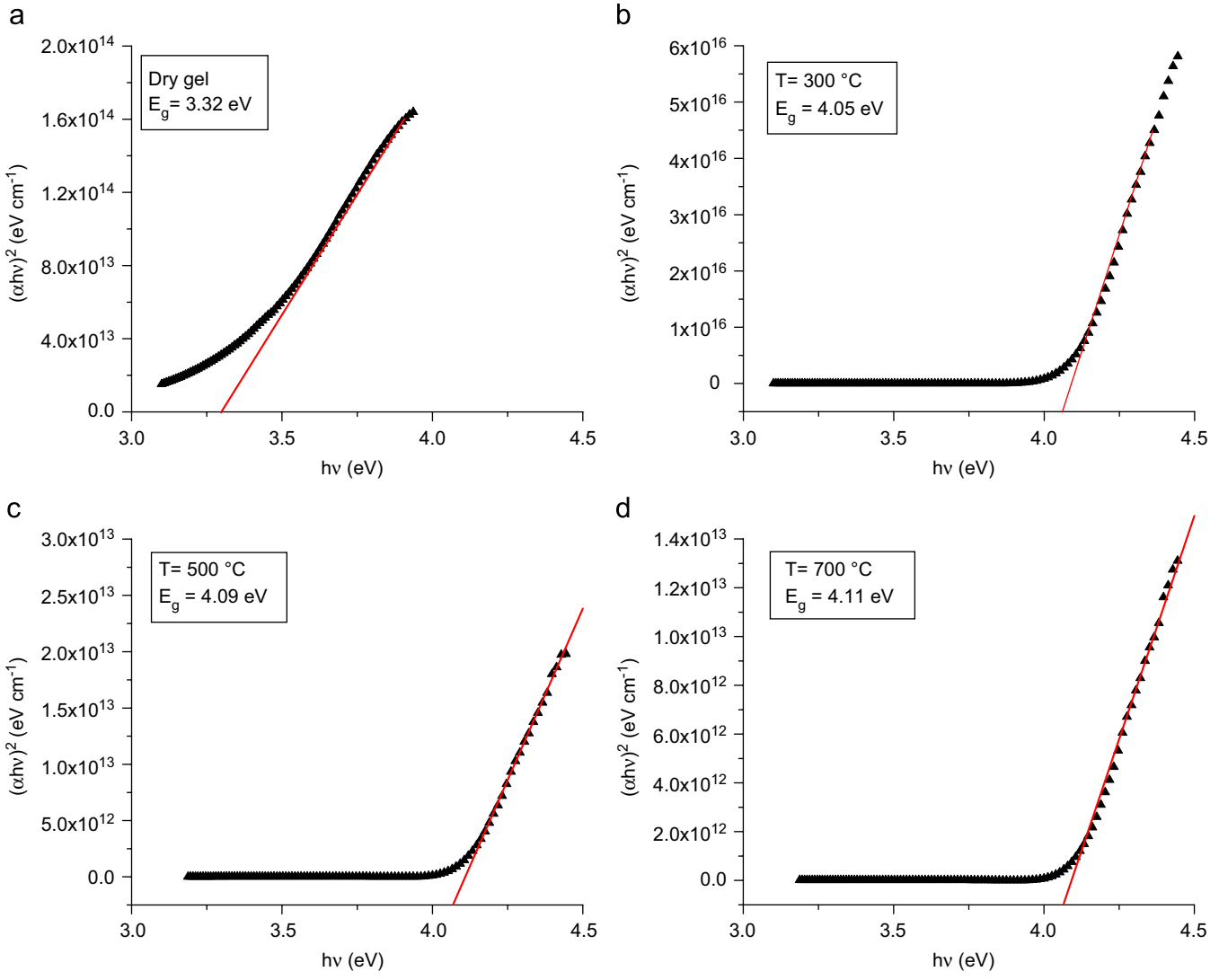

Fig. 6. The plot of $(\alpha h\nu)^2$ versus $h\nu$ to determine the band gap of SnO_2 nano-particles at various annealing temperatures, (a) dry gel-powder, (b) 300 °C, (c) 500 °C and (d) 700 °C.

4. Conclusions

Tin oxide nano-particles were synthesized successfully by the polymerizing–complexing sol–gel method. Based on XRD and TEM studies, using citrate acid as a complexing agent in the synthesis of SnO_2 nano-particles was effective to prevent the grain growth or agglomeration of particles, and the addition of ethylene glycol as polymerization agent to the precursor solution led to a homogeneous distribution of particles. The post-annealing results on nano-particles show that at high annealing temperatures, especially above 500 °C, all the organic additives are removed from the powders, and crystalline SnO_2 nano-particles are formed. The mean size range of particles (by XRD patterns) was between 5 and 18 nm, depending on the annealing temperatures. The optical direct band gap values of SnO_2 nano-particles have slowly changed from 4.05 to 4.11 eV by increasing the annealing temperature from $T = 300$ to 700 °C. These values exhibit nearly a 0.5 eV blue shift in E_g from that of bulk SnO_2 (3.6 eV), which is related to the size decrease of the particles and to the quantum confinement limit reaching of nano-particles.

Considering these results, the most suitable annealing temperature for preparation of SnO_2 nano-powder is 500 °C, and the PC sol–gel method is very efficient for the preparation of homogeneous SnO_2 nano-particles for nano-sensors, ceramic and other industrial applications.

Acknowledgments

The authors would like to thank Mrs. M. Hassanzadeh from Solid State Physics Research Center, Damghan University of Basic Sciences for XRD analyses and Mrs. R. Pesyan from Central Research Laboratory of Ferdowsi University of Mashhad for TEM analysis.

References

[1] M. Bhagwat, P. Shah, V. Ramaswamy, Mater. Lett. 57 (2003) 1604.
[2] B.G. Lewis, D.C. Paine, MRS Bull. 25 (8) (2000) 22.
[3] H.L. Hartnagel, A.L. Dawar, A.K. Jain, C.J. Jagadish, Semiconducting Transparent Thin Films, IOP, Bristol, 1995.
[4] M. Shoyama, N. Hashimoto, Sensor. Actuat. B 93 (2003) 585.
[5] X. Yuan, L. Cao, H. Wan, G. Zeng, S. Shiquan, Thin Solid Films 327–329 (1998) 33.
[6] L.R.B. Santos, T. Chartier, C. Pagnoux, J. Eur. Ceram. Soc. 24 (2004) 3713.
[7] C. Premakumara, M. Kakihana, M. Yoshimura, Solid State Ionics 108 (1998) 23.
[8] J. Zhang, L. Gao, J. Solid State Chem. 177 (2004) 1425.
[9] N. Segent, P. Gelin, L. Perrier, H. Praliaud, G. Thomas, Sensor. Actuat. B 84 (2002) 76.
[10] C. Ararat Ibarguen, A. Mosquera, R. Parra, Mater. Chem. Phys. 101 (2007) 433.
[11] N.S. Baik, G. Sakai, N. Miura, N. Jamazoe, J. Am. Ceram. Soc. 83 (2000) 983.
[12] M. Ristic, M. Ivanda, S. Popovic, S. Music, J. Non-Cryst. Solids 303 (2002) 270.
[13] F. Paraguay-Delgado, W. Antunez-Flores, M. Miki-Yoshida, A. Aguilar-Elguezabal, P. Satiago, R. Diaz, J.A. Ascencio, Nanotechnology 16 (2005) 694.
[14] M. Kakihana, J. Sol–Gel Sci. Technol. 6 (1996) 7.
[15] M.P. Pechini, U.S. Patent, July 1967.
[16] E.R. Leite, A.P. Maciel, I.T. Weber, P.N.L. Filho, E. Longo, C.O.P. Santos, A.V.C. Andrae, C.A. Pakoscimas, Y. Manietle, W.H. Schreiner, Adv. Mater. 14 (2002) 5.
[17] C.M. Liu, X.T. Zu, Q.M. Wei, L.M. Wang, J. Phys. D: Appl. Phys. 39 (2006) 2494.
[18] H. Zhu, D. Yang, G. Yu, H. Zhang, K. Yao, Nanotechnology 17 (2006) 2386.